

Effect of spin-system fluctuations on heat transport in RbMnF_3 close to the Néel temperature

M. Marinelli,* F. Mercuri, and S. Foglietta

*Dipartimento di Ingegneria Meccanica, II Università di Roma "Tor Vergata" and Sezione INFM Roma II,
Via della Ricerca Scientifica, 00133 Roma, Italy*

D. P. Belanger

Department of Physics, University of California, Santa Cruz, California 95064

(Received 7 February 1996)

The photopyroelectric technique has been used to simultaneously study the critical behavior of the specific heat, thermal conductivity, and thermal diffusivity at the antiferromagnetic-paramagnetic phase transition of RbMnF_3 . It has been shown that the critical exponent of the diffusivity is equal to the specific heat one. This result, together with the ones already reported for Cr_2O_3 and FeF_2 at the same transition, shows that there is no influence of the uniaxial anisotropy field on the critical behavior of the thermal diffusivity. A broad cusplike maximum has been found in the thermal conductivity close to the Néel temperature. It has been attributed to the decreasing importance of the scattering of phonons by the spin fluctuation with respect to other nonmagnetic scattering processes once the transition temperature is approached. [S0163-1829(96)00229-9]

I. INTRODUCTION

An interesting point in the study of the critical behavior of the thermal conductivity (k) and thermal diffusivity ($D = k/\rho c$, where c is the specific heat and ρ is the density) is the one regarding the effect of critical fluctuations in the spin system close to a magnetic phase transition. The spin-phonon coupling in magnetic materials is usually small, and therefore high-resolution techniques are needed for experimental investigations. It has been recently shown¹ that photothermal techniques can be used for high-resolution measurements of thermal parameters. The photopyroelectric configuration, in particular, has been used to simultaneously monitor the critical behavior of c , k , and D close to antiferromagnetic-paramagnetic (AF) phase transition of uniaxial magnetic insulators.^{2,3} A question may arise whether the uniaxial anisotropy field has an effect on the critical behavior of the dynamic thermal parameters close to the AF transition. No theoretical predictions are at present available for the critical behavior of k and D in isotropic systems, while in the case of uniaxial systems there is a theoretical prediction⁴ which has been recently confirmed in the case of FeF_2 .³

In the present paper we shall report on high-resolution simultaneous measurements of the specific heat, thermal conductivity, and thermal diffusivity at the antiferromagnetic-paramagnetic phase transition of RbMnF_3 . This compound is a well-known isotropic antiferromagnet and probably the closest realization of a three-dimensional (3D) Heisenberg antiferromagnet. The obtained specific heat data are in close agreement with high-resolution data available in the literature⁵ and with the theoretical predictions of the 3D Heisenberg model. The thermal diffusivity shows a dip at T_N and a critical exponent b , which is approximately equal the specific heat one α . The thermal conductivity shows a broad peak around T_N , which is attributed to the effect of spin-phonon scattering on the heat transport process. Since these results are similar to the ones obtained in the case of the uniaxial FeF_2 ,³ where $b = -\alpha$ and a broad

peak was observed in k around T_N , it seems that the uniaxial anisotropy plays no appreciable role.

II. SAMPLE CHARACTERISTICS

RbMnF_3 has a cubic perovskite structure with a lattice constant $a = 4.218 \text{ \AA}$,⁶ which is maintained at all temperatures.⁷ With respect to other antiferromagnets, it has only a small anomaly in the thermal expansion at T_N , which indicates a stable lattice structure.⁸ The density is 4.317 g/cm^3 at room temperature.⁹ The magnetic uniaxial anisotropy field $H_A = 4.5 \text{ Oe}$ (Ref. 10) is very small if compared to the exchange field, the ratio of the two being 6×10^{-6} .¹¹ This is due to the fact that the Mn^{2+} cation has no orbital moment and there is no dipolar interaction because of the cubic structure of the site. RbMnF_3 can therefore be well described by a Heisenberg Hamiltonian with a nearest-neighbor interaction. Spin-wave dispersion measurements showed that the nearest-neighbor exchange constant is $J = 0.29 \pm 0.03 \text{ meV}$, while the second neighbor constant has a value of less than 0.02 meV .¹² The Heisenberg-like behavior in the vicinity of T_N has been confirmed by many experimental results. Specific heat measurements gave $\alpha = -0.14 \pm 0.01$ with an amplitude ratio $A^+/A^- = 1.40 \pm 0.04$.⁵ This value agrees quite well the theoretical predictions of the 3D Heisenberg model where $\alpha = -0.115 \pm 0.009$ (Ref. 13) and $A^+/A^- = 1.58$.¹⁴ Similar agreement has been found for the critical exponents $\eta = 0.055 \pm 0.010$, $\nu = 0.701 \pm 0.011$, and $\gamma = 1.366 \pm 0.024$, obtained from neutron scattering experiments,¹⁵ and the theoretical predictions. Ultrasound measurements showed a peak at T_N in the absorption coefficient and a velocity shift.¹⁶ Since in RbMnF_3 ultrasounds interact essentially with the energy density fluctuations in the spin system and not with the order parameter fluctuations, a spin-lattice relaxation time has been calculated. The theoretical prediction is in excellent agreement with the experimental observation.¹⁷ It has been also shown that in this compound the strongest coupling for phonons with frequencies of the order of 100 MHz

is via the strain dependence of the exchange integral (volume magnetostriction).¹⁸ Thermal conductivity data do not show evidence of a magnon contribution to the heat transport.⁹ It has been shown that this result can be strongly affected by the presence of impurities in the sample.¹⁹ A flat k behavior has been reported close to T_N .⁹ The resolution of the measurement was, however, very poor since data were collected every 1–2 K.

III. EXPERIMENT

The experimental configuration we have used is a standard back detection photopyroelectric one.¹ The sample, usually in the form of a thin slab, is heated on one side by a modulated heating source, and the temperature oscillations at the opposite side were detected by means of a pyroelectric transducer. In the present work we used as a heating source a 100-mW Ar⁺-ion laser emitting at 514 nm, acousto-optically modulated at 27 Hz. Since RbMnF₃ is transparent in the visible, one surface was coated with a 200-nm-thick Ti overlayer. The sample was in thermal contact with the transducer through a very thin silicone grease layer. The influence of the silicone grease and of the Ti layer was negligible. The transducer we used was a 300- μ m-thick, Z-cut, LiTaO₃ pyroelectric crystal and the signal was analyzed by means of a lock-in amplifier. It has been shown¹ that if the sample and transducer are optically opaque and thermally thick, c , k , and D can be determined simultaneously provided that the sample density and transducer properties are known. Only two of the above-mentioned thermal parameters can be obtained from the measurements while the third is calculated from the relation $D = k/\rho c$. In the following we shall assume that the sample density is constant over all of the investigated temperature region. This assumption seems quite reasonable in view of the already mentioned thermal expansion data that show a very stable lattice structure. The sample plus transducer assembly was mounted in a variable-temperature cryostat, and the temperature rate change was 50 mK/min. We could vary the light intensity reaching the sample using a negative lens. The temperature variation rate and the light intensity were decreased down to values for which further decrease did not cause any variation in the experimental results. This was done to keep as low as possible the thermal gradients introduced in the sample. The spread of the heating light over the sample surface obtained with the negative lens also ensured a one-dimensional geometry, since the spot size and therefore the heated area were much larger (≈ 1 cm) than the sample thickness.

IV. EXPERIMENTAL RESULTS

Figure 1 shows the specific heat data in the temperature range 79–89 K compared with some selected data points taken from Ref. 5. The calibration of our setup has been performed at 88 K using the specific heat reported at the same temperature in Ref. 5 and the determination of the absolute value of the thermal diffusivity which has been obtained by a frequency scan² at the same temperature. The two data sets superimpose quite well over the whole temperature range. The agreement gives an idea of the quality of the measurement for the specific heat, but the same consider-

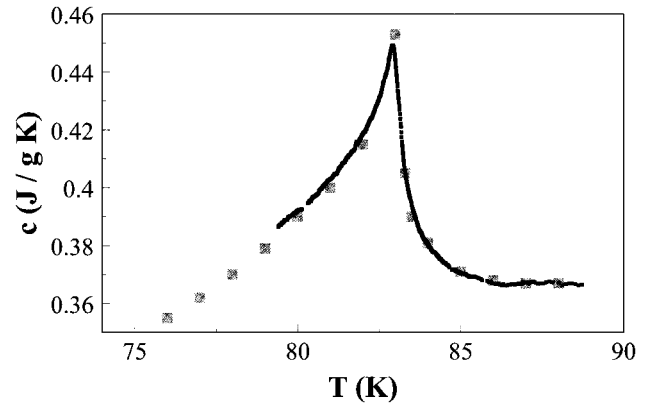


FIG. 1. Specific heat data vs temperature. (■) are specific heat data taken from Ref. 5.

ation can be extended to dynamic quantities as well since they are measured simultaneously. We have tried to run measurements at different frequencies within a frequency range where the thermally thick condition for the sample is still valid, but we did not observe any significant change in the data.

Figure 2 shows the thermal diffusivity data that show a dip at T_N due to the critical slowing down. Very similar behaviors have been obtained for the uniaxial antiferromagnets Cr₂O₃ (Ref. 2) and FeF₂.³

Figure 3 shows the thermal conductivity data. A broad peak is clearly visible close to T_N . The effect of thermal gradients in the sample generally results in a rounding of the signal amplitude and phase close to the transition temperature. This rounding can produce artifacts in the thermal conductivity as shown in Ref. 3. Specific heat and thermal diffusivity data show that this rounding, if present, is confined in a temperature region very close to T_N (tens of mK), and therefore the broad peak in k , whose width is about 2 K around T_N , cannot be an artifact due to the thermal gradients.

V. DATA ANALYSIS

A. Fitting functions

To fit the specific heat data we choose the expression

$$c_p = B + E(T - T_N) + A^\pm |T - T_N|^{-\alpha} (1 + D^\pm |T - T_N|^{0.5}), \quad (1)$$

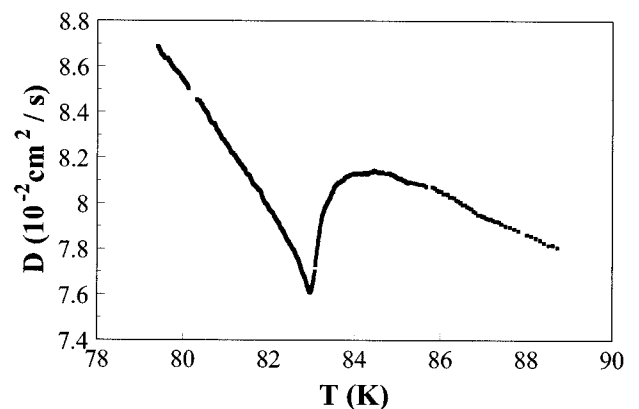


FIG. 2. Thermal diffusivity vs temperature.

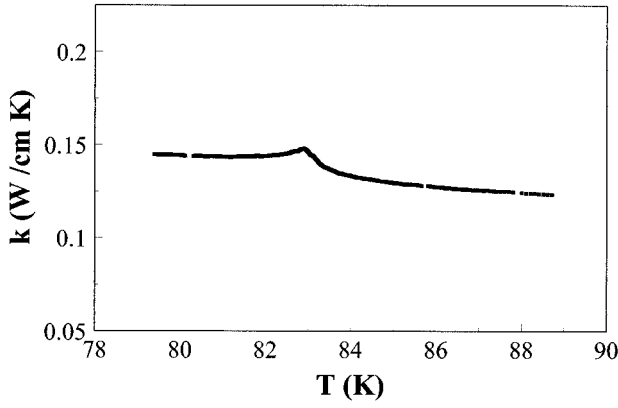


FIG. 3. Thermal conductivity vs temperature.

where \pm refers to $T > T_N$ and $T < T_N$, respectively. In the case of the thermal conductivity, we decided to fit the $1/k$ data instead of the k ones with the expression

$$1/k = 1/k_{\text{nonmag}} + 1/k_{\text{mag}} = L + M(T - T_N) + N^{\pm} |T - T_N|^{-g} \times (1 + H^{\pm} |T - T_N|^{0.5}). \quad (2)$$

The reason for this choice relies on the fact that all the thermal resistances associated with the various heat conduction mechanisms in the system under investigation are in series. In this way the singular term in the fitting function can be easily related to the magnetic contribution to the heat conduction processes. It must be noted, however, that the magnetic contribution cannot be easily separated from the non-magnetic ones. As an example, let us consider the case of a cusplike maximum in k . In this case the singular term in Eq. (2) will have a positive amplitude and a negative exponent and will go to zero approaching T_N . This means that the constant and linear terms will account for a magnetic contribution, even away from T_N , which cannot be evaluated. A correction-to-scaling term similar to the one used for c_p has been included in the fitting function.

If we combine Eqs. (1) and (2) to obtain the thermal diffusivity from the equality $D = k/\rho c$, it turns out that the singular behavior of D will be described by a complicated combination of singular terms coming from c and k . This makes the comparison with theoretical predictions, when available, very difficult. As an example, let us consider a model for critical dynamics which includes a purely diffusive heat conduction mode. The characteristic frequency (inverse of the relaxation rate) of such a mode is $\omega_E \propto D_{\text{sing}} \omega^2 \propto q^{z_E}$, where q is the mode wave vector and D_{sing} is the singular part of the thermal diffusivity. Applying the dynamic scaling hypothesis²⁰ and assuming $D_{\text{sing}} \propto |T - T_N|^{-b}$, we obtain $\omega_E \propto D_{\text{sing}} q^2 \propto \xi^{b/\nu} q^2 = (q\xi)^{b/\nu} q^{2-b/\nu}$ and therefore $z_E = 2 - b/\nu$, where ξ is the correlation length and ν is its critical exponent. In a few cases there are theoretical predictions for z_E as in the case of the so-called model C,²¹ where $z_E = 2 + \tilde{\alpha}/\nu$, where $\tilde{\alpha} = \max(\alpha, 0)$, and therefore a prediction for b ($b = -\alpha$) can be obtained. It must be pointed out that the simple relation for α and b follows from the assumption we have made about D_{sing} . If we choose to obtain D from Eq. (1), Eq. (2), and the equality $D = k/\rho c$, we shall end up with a complicated relation between α and the singular terms

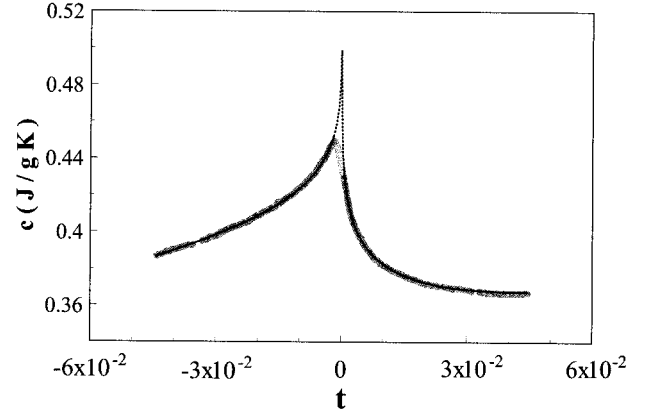


FIG. 4. Specific heat data vs reduced temperature $t = (T - T_N)/T_N$. The solid curve corresponds to the best-fit curve. The dotted line corresponds to the reduced temperature region, which has not been considered in the fit.

coming from c and k . It is therefore much more convenient to choose an expression for D of the form

$$D = D_{\text{reg}} + D_{\text{sing}} = V + W(T - T_N) + U^{\pm} |T - T_N|^{-b} \times (1 + F^{\pm} |T - T_N|^{0.5}). \quad (3)$$

Equation (3) has been already used to fit the diffusivity data of Cr_2O_3 and FeF_2 , and the choice we have made in the present paper allows a comparison of the critical behavior of D between RbMnF_3 and the above-mentioned compounds. The fitting procedure for c , $1/k$, and D is the same as in Ref. 2.

B. Results

The best-fit curve and the corresponding experimental data for the specific heat are shown in Fig. 4. The results of the fit are shown in Table I. The critical exponent $\alpha = -0.11 \pm 0.01$ is in good agreement with the Heisenberg prediction -0.115 ± 0.009 .¹³ The amplitude ratio is consistent, within the statistical uncertainties, with the one reported in Ref. 5, the two being systematically smaller than the expected value of 1.58.¹⁴ Our fit has been obtained with the constraint $B^+ = B^-$, which is expected from the theory, while in Ref. 5, B^+ and B^- were significantly different. The correction-to-scaling terms are small, and a good fit could be obtained putting $D^+ = D^- = 0$. A ratio value $D^+/D^- = 1.4$ is expected for a 3D Heisenberg system,¹⁴ but our results do not fit this prediction. This is probably due to the rather large statistical uncertainties that make the above-mentioned comparison unreliable.

Figure 5 shows the best-fit curve for $1/k$ contrasted with the corresponding experimental data. The fit results are reported in Table I. The singular term has a positive amplitude and a negative exponent. This means that k has a cusplike maximum and not a divergence.

Figure 6 shows the best-fit curve for D and the experimental data, and again the fit results are reported in Table I. Since D shows a dip at T_N , it must have a cusplike behavior and this is the reason for the constraint $b < 0$.

TABLE I. Values of the adjustable fitting parameters for the specific heat, thermal diffusivity, and inverse of the thermal conductivity obtained with Eqs. (1), (2), and (3).

	α	A^+/A^-	T_c (K)	B (J/g K)	E (J/g K)	A^- (J/g K)	D^-	D^+	χ_v^2
c (J/g K)	-0.11 ± 0.01	1.27 ± 0.09	83.07 ± 0.03	0.60 ± 0.01	0.006 ± 0.005	-0.18 ± 0.01	-0.005 ± 0.005	-0.003 ± 0.005	1.03
	b	U^+/U^-	T_c (K)	V (cm ² /s)	W (cm ² /s)	U^- (cm ² /s)	F^-	F^+	χ_v^2
D (cm ² /s)	-0.11 ± 0.02	1.27 ± 0.09	83.07 ± 0.02	0.067 ± 0.008	-0.003 ± 0.002	0.011 ± 0.001	-0.2 ± 0.3	0.2 ± 0.3	0.97
	g	N^+/N^-	T_c (K)	L (cm K/W)	M (cm K/W)	N^- (cm K/W)	H^-	H^+	χ_v^2
$1/k$ (cm K/W)	-0.08 ± 0.04	1.1 ± 0.2	83.05 ± 0.08	4.2 ± 0.3	0.04 ± 0.02	3.0 ± 0.2	-0.07 ± 0.05	-0.01 ± 0.04	1.01

VI. DISCUSSION

In the next subsections we will make a comparison with other experimental results and existing theories.

A. Thermal diffusivity

A few considerations can be drawn from the experimental results up to now available on the critical behavior of the thermal diffusivity at the AF phase transition. Data are available for FeF₂,³ which is a quasi-ideal Ising-like system, for RbMnF₃, which is a quasi-ideal Heisenberg-like system, and for Cr₂O₃,² which shows a crossover from Heisenberg to Ising-like behavior approaching T_N . The b critical exponent is approximately the same in all the three above-mentioned compounds since $b = -0.11 \pm 0.02$ for FeF₂, $b = -0.09 \pm 0.01$ for Cr₂O₃ with $t = |T - T_N|/T_N < 10^{-3}$ and $b = -0.11 \pm 0.02$ for RbMnF₃. This means that the uniaxial anisotropy field does not play any role on the critical behavior of the thermal diffusivity. From the analysis of the data, it follows that the critical exponents for D and c obey, in these antiferromagnetic insulators, the relation $b = -|\alpha|$. The relation follows empirically from the experimental data and has, up to now, no theoretical justification. It is plausible, however, that, since we have seen that the singularity in k is quite small and $D = k/\rho c$, the result $b = -|\alpha|$ for all the cases

investigated so far is a consequence of the cusp in c for the Heisenberg case and the divergence in c for the Ising case. With the Heisenberg case, the contribution to c from the singular term vanishes as the reduced temperature t approaches zero. Hence D , which is nearly proportional to the inverse of c , will exhibit a nonsingular background and a singular term, which is a cusp. The singular term will have the same exponent as c , i.e., $b = \alpha = 0.11$. In contrast, for the Ising case the singular term is divergent. D is dominated by the singular term as t approaches zero and will exhibit inverse singular behavior with a nonsingular background, i.e., $b = -\alpha = -0.11$. Since α for the Heisenberg case is nearly equal in magnitude, but opposite in sign to the Ising case, the inverse shows little change as the uniaxial anisotropy increases. This view is further supported by the amplitude ratios. For the Heisenberg case we see that D has the same amplitude ratio as c , whereas for the Ising case, the amplitude ratio for D is approximately the inverse of that for c . It is interesting to note that the equality is obeyed even if the obtained k behaviors in the vicinity of T_N are rather different. In the case of Cr₂O₃, a small discontinuity and a change in slope have been found at T_N , while in the case of FeF₂ and RbMnF₃, a broad peak around T_N , whose width was about 5 and 2 K, respectively, was found. This means that short-range processes, such as the scattering of phonons, do not influence significantly the D critical behavior. This could

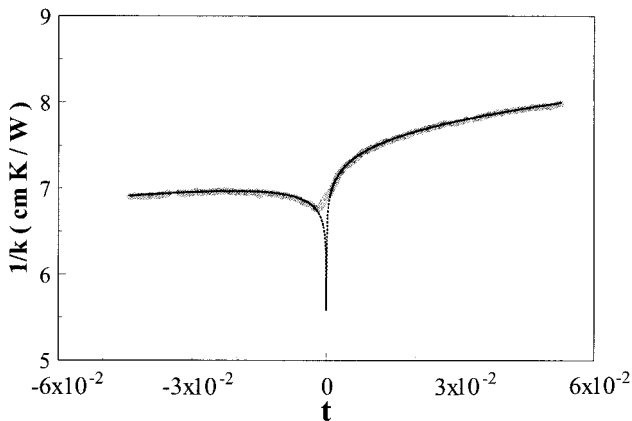


FIG. 5. $1/k$ vs reduced temperature $t = (T - T_N)/T_N$. The solid curve corresponds to the best-fit curve. The dotted line corresponds to the reduced temperature region, which has not been considered in the fit.

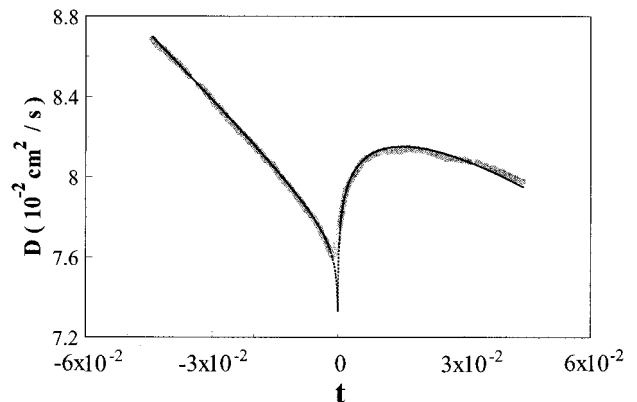


FIG. 6. Thermal diffusivity data vs reduced temperature $t = (T - T_N)/T_N$. The solid curve corresponds to the best-fit curve. The dotted line corresponds to the reduced temperature region, which has not been considered in the fit.

be due to the weak spin-phonon coupling and could also be an important key point in the development of a general theory of critical behavior of dynamic thermal parameters.

B. Thermal conductivity

The results obtained for k can be more easily discussed in terms of phonon scattering mechanisms, each of them responsible for a given contribution to the total thermal resistance. It follows that $1/k = 1/k_{(\text{nonmag})} + 1/k_{(\text{mag})}$ where “nonmag” refers to phonon-phonon scattering, umklapp, scattering with impurities, etc., while “mag” refers to the spin-phonon coupling mechanisms. The magnetic resistive term originates from the spin-lattice interaction¹⁷ and close to T_N from an additional term that accounts for phonon scattering by critical fluctuations of the order parameter. A weak spin-phonon coupling will result in a small $1/k_{(\text{mag})}$, and therefore the thermal conductivity will be dominated by nonmagnetic scattering processes. This is the reason why a high-resolution technique is needed to detect a variation in k in the vicinity of a magnetic phase transition. The poor resolution was probably the reason why Gustafson and Walker⁹ did observe a flat k behavior for RbMnF₃ around T_N . They collected data every 1–2 K, and they had therefore no chance to observe the peak we have obtained, which has a width of about 2 K. It should be noted that a peak in k similar to the one reported in this paper for RbMnF₃ has been found in FeF₂³ where a sharp anomaly in k in a temperature region of about 30 mK around T_N superimposed on a broad peak has been found. The sharp anomaly was in that case attributed to thermal gradients in the sample. No peak, but rather a small discontinuity, in k has been found in the case of Cr₂O₃ at T_N .² The transition temperature in this case was 307.26 K. In this temperature region, however, the magnetic scattering will be probably completely masked by other nonmagnetic scattering mechanisms. A decrease is in fact expected in the relaxation times associated with nonmagnetic scattering processes close to room temperature.

There are not very many high-resolution data on the critical behavior of k available in the literature, and this is partially due to some experimental difficulties. A thermal gradient must be introduced in the sample during the measurement, and this tends to average the output over an important region close to the transition temperature. Flat k behavior as well as a dip in the thermal conductivity close to a magnetic phase transition has been reported in different compounds. A dip was observed in the two ferromagnets CuK₂Cl₄·2H₂O (Ref. 22) and EuO.²³ The origin of such a dip was attributed to the increasing importance of phonon scattering by the fluctuations in the spin system once the transition temperature is approached. In the case of EuO, however, the accuracy of the above-mentioned result has been questioned and a rather flat k behavior was reported later on.²⁴ Similar smooth k behavior was also found in the antiferromagnet CoO.²⁴ These results were explained in terms of the usually small spin-phonon coupling that makes the spin-phonon contribution negligible with respect to the other phonon scattering mechanisms. More recently a dip in k was reported for Gd,²⁵ but as a result of the complexity of the system, where electrons also contribute to the heat transport, no definite conclusion could be drawn on the physical mechanism responsible for such behavior. In summary, the

critical behavior of k seems to show a system dependence that is probably due to the different spin-phonon coupling mechanisms that are present in particular compounds.

C. Comparison with existing theories

Existing theories on the critical behavior of dynamic thermal parameters are largely incomplete. Kawasaki observed that since the heat transport is dominated by short-range processes such as phonon scattering, no divergence should be expected for D and k .²⁶ Moreover, since these effects are system dependent, he suggested that the scaling laws may not hold for heat transport.²⁶ These arguments and the above-mentioned small spin-phonon coupling are the reasons why in modern theories of critical phenomena the heat transport has been largely ignored. The result is that even in the simple case of a magnetic insulator it is not clear what behavior for k and D should be expected close to the transition temperature.

Thermal diffusivity

The fit results show that thermal diffusivity can be fitted with a critical exponent $b = \alpha$. It has been shown that in the case of the Ising-like system FeF₂ the prediction of model C, $b = -\alpha$, was confirmed by experimental results.³ In the case of RbMnF₃ the appropriate dynamic model should be model G in which an additional long-lived mode corresponding to the long-wavelength components of the spin wave have been included.⁴ The heat conduction mode has not been considered in model G, and therefore the experimental result $b = \alpha$ cannot be contrasted with any theoretical prediction.

Thermal conductivity

As already stated, a theoretical model for the thermal conductivity behavior close to a magnetic phase transition must consider the different spin-phonon coupling mechanisms that are relevant in the system under investigation. Bearing in mind that existing theories are largely incomplete, we can try to compare our experimental results with some predictions by Kawasaki for the propagation of high-frequency phonons close to a magnetic phase transition²⁷ in systems where the spins couple with the phonons via the volume magnetostriction. Let us assume that $k \propto L$, where L is the phonon mean free path. As for k , L can be considered the sum of several contributions so that $1/L = 1/L_{(\text{nonmag})} + 1/L_{(\text{mag})}$. The observed cusp maximum in k , following our assumption, means a cusp maximum in L and therefore a singular contribution which vanishes at T_N . It has been shown²⁷ that the critical part of the attenuation coefficient for high-frequency ultrasounds, in the case of volume magnetostrictive spin-phonon coupling, can be written as

$$\alpha(\omega) = \frac{|T - T_N|^{2(w-\alpha)}}{T_N} \omega^{1+\alpha/\nu\theta},$$

where w is a small positive number and θ is a parameter characteristic of the system under investigation. $\alpha(\omega)$ decreases approaching T_N . Now assuming that this result, obtained for high-frequency phonons, can be extended to thermal phonons and assuming also that $\alpha \sim 1/L_{(\text{mag})}$, $L_{(\text{mag})}$ must increase, therefore producing an increase in k close to T_N .

The above-mentioned assumptions seem to be realistic in RbMnF_3 (Ref. 12) and FeF_2 (Ref. 28) since the exchange interactions extend mainly to nearest neighbors and therefore fluctuation in the order parameter (staggered magnetization) can couple only with high-frequency phonons. The prediction by Kawasaki has been obtained considering that the spin-phonon coupling occurs mainly via the volume magnetostriction. This seems to be the case of RbMnF_3 , at least in the case of low-frequency phonons (100 MHz).¹⁸ The comparison with the Kawasaki prediction cannot be made more quantitative because of the many assumptions and the poor accuracy in the determination of the value of the critical exponent in Ref. 27.

VII. CONCLUSIONS

It has been shown that in RbMnF_3 the critical exponent for the thermal diffusivity b is equal to the specific heat one α . This result, compared with the results already reported for Cr_2O_3 (Ref. 2) and FeF_2 ,³ leads to the conclusion that in these antiferromagnetic insulators at the AF phase transition the two exponents are connected by the empirical relation $b = -|\alpha|$. In the above-mentioned compounds, the critical exponent for D is approximately the same and this means

that the uniaxial anisotropy field has no effect on the thermal diffusivity critical behavior. The amplitude ratios also do not change appreciably with the uniaxial anisotropy. The fact that neither the exponent nor amplitude change with uniaxial anisotropy is probably a consequence of the fact that the conductivity singularity is small and the diffusivity is therefore approximately inversely proportional to the specific heat.

A broad peak, similar to the one already reported for FeF_2 , has been obtained for k . This peak has been attributed to the decreasing importance of the magnetic scattering of phonons by the spin system with respect to nonmagnetic scattering mechanisms once the transition temperature is approached. This peak in k has not been observed in Cr_2O_3 , but this is probably due to the relatively high T_N of this compound, which makes nonmagnetic scattering processes dominant with respect to the magnetic ones.

ACKNOWLEDGMENTS

We would like to thank Professor B. I. Halperin and D. L. Huber for a very fruitful discussion during the preparation of the manuscript. This research was supported in part by INFN of Italy and DOE Grant No. DE-FG03-87ER54324.

*Electronic address: marinelli@utovrm.it

- ¹M. Marinelli, U. Zammit, F. Mercuri, and R. Pizzoferrato, *J. Appl. Phys.* **72**, 1096 (1992).
- ²M. Marinelli, F. Mercuri, U. Zammit, R. Pizzoferrato, F. Scudieri, and D. Dadarlat, *Phys. Rev. B* **49**, 9523 (1994).
- ³M. Marinelli, F. Mercuri, and D. P. Belanger, *Phys. Rev. B* **49**, 8897 (1995).
- ⁴P. C. Hohenberg and B. I. Halperin, *Rev. Mod. Phys.* **49**, 435 (1977).
- ⁵A. Kornblitt and G. Ahlers, *Phys. Rev. B* **8**, 5163 (1973).
- ⁶L. J. de Jongh and A. R. Miedema, *Adv. Phys.* **23**, 1 (1974).
- ⁷D. T. Teaney, V. L. Moruzzi, and B. W. Argyle, *J. Appl. Phys.* **9**, 212 (1962).
- ⁸F. P. Jona and G. Shirane, *Ferroelectric Crystals* (Pergamon, New York, 1962).
- ⁹J. Gustafson and T. Walker, *Phys. Rev. B* **8**, 3309 (1973).
- ¹⁰D. T. Teaney, M. J. Freiser, and R. W. H. Stevenson, *Phys. Rev. Lett.* **9**, 212 (1962).
- ¹¹M. J. Freiser, P. E. Seiden, and D. T. Teaney, *Phys. Rev. Lett.* **10**, 293 (1963).
- ¹²C. G. Windsor and R. W. H. Stevenson, *Proc. Phys. Soc. (London)* **87**, 501 (1966).
- ¹³J. C. Le Guillou and J. Zinn-Justin, *Phys. Rev. B* **21**, 3976 (1980).
- ¹⁴V. Privman, P. C. Hohenberg, and A. Aharony, in *Phase Transitions and Critical Phenomena*, edited by C. Domb and J. L. Lebowitz (Academic, New York, 1991), Vol. 14.
- ¹⁵A. Tucciarone, H. Y. Lau, L. M. Corliss, A. Delapalme, and J. M. Hastings, *Phys. Rev. B* **4**, 3206 (1971).
- ¹⁶T. J. Moran and B. Luthi, *Phys. Rev. B* **4**, 122 (1971).
- ¹⁷D. L. Huber, *Phys. Rev. B* **3**, 836 (1971).
- ¹⁸B. Luthi, P. Papon, and R. J. Pollina, *J. Appl. Phys.* **40**, 1029 (1969).
- ¹⁹J. B. Hartmann, *Phys. Rev. B* **15**, 273 (1977).
- ²⁰B. I. Halperin and P. C. Hohenberg, *Phys. Rev.* **177**, 952 (1969).
- ²¹B. I. Halperin, P. C. Hohenberg, and S. Ma, *Phys. Rev. B* **10**, 139 (1974).
- ²²G. S. Dixon and D. Walton, *Phys. Rev.* **185**, 735 (1969).
- ²³R. G. Morris and J. L. Cason, *Helv. Phys. Acta* **41**, 1045 (1968).
- ²⁴M. B. Salamon, P. R. Garnier, B. Goulding, and E. Buehler, *J. Phys. Chem. Solids* **35**, 851 (1974).
- ²⁵C. Glorieux, J. Thoen, G. Bednarz, M. A. White, and D. J. W. Geldart, *Phys. Rev. B* **52**, (1995).
- ²⁶K. Kawasaki, *Prog. Theor. Phys. (Kyoto)* **40**, 706 (1968).
- ²⁷K. Kawasaki, *Int. J. Magn.* **1**, 171 (1971).
- ²⁸M. T. Hutchings, B. D. Rainford, and H. J. Guggenheim, *J. Phys. C* **3**, 307 (1970).